Eur. Phys. J. AP **3**, 309–320 (1998)

THE EUROPEAN PHYSICAL JOURNAL APPLIED PHYSICS

Rheological modeling of complex fluids: III. Dilatant behavior of stabilized suspensions

D. Quemada[a]

Laboratoire de Biorhéologie et d'Hydrodynamique Physico-chimique, Université Denis Diderot (Paris 7)[b] LBHP, case 7056, Université Paris 7, 2 place Jussieu, 75251 Paris Cedex 05, France

Received: 11 March 1998 / Revised and Accepted: 2 June 1998

Abstract. A new structural model of shear-thickening "dilatancy" is proposed for (strongly) stabilized disperse systems. This model is based on the effective volume fraction (EVF) concept, developed in Part I of this series and previously used for the rheological modeling of complex fluids. In such a description, the latter are considered as concentrated dispersions of basic structural units (SUs) — either small, compact clusters or primary particles —, forming large structures at low shear. As shear rate increases, rupturing of these large structures leads to the shear thinning observed prior to dilatancy. The novelty of this model lies in assuming that, beyond the onset of dilatancy, hydrodynamic forces promote, at the expense of basic-SUs, the formation of *hydrodynamic clusters* as both rheo-optical experiments and numerical simulations recently demonstrated, in contradiction with the (classical) theory based on a shear induced disruption of particle layering. Dilatancy directly results from the increase of the EVF of the dispersion, closely related to the increasing volume of continuous phase imprisoned inside hydroclusters whose size grows as the shear rate increases. Predictions of the model are discussed in comparison with the main features observed in a large number of dilatant dispersions, especially the volume fraction dependences of viscosity and critical shear rates (onset of dilatancy, maximum and discontinuity in viscosity) also the effects of particle size, polydispersity and suspending fluid viscosity.

Résumé. On propose un nouveau modèle structurel du rhéo-épaississement "dilatance" dans les systèmes dispersés fortement stabilisés. Ce modèle est basé sur le concept de fraction volumique effective (FVE), développé dans la partie I de ce travail et utilisé précédemment pour la modélisation rhéologique des fluides complexes, ces derniers étant considérés comme des dispersions concentrées d'unités structurelles de base (US) — soit de petits amas compacts, soit des particules primaires —, formant de grandes structures à faible cisaillement. Lorsque la vitesse de cisaillement augmente, la rupture de ces grandes structures conduit au comportement rhéofluidifiant observé avant l'apparition de la dilatance. La nouveauté de ce modèle résulte de l'hypothèse suivante : au-delà du seuil de dilatance, les forces hydrodynamiques provoquent, aux dépens des US de base, la formation d'*amas hydrodynamiques*, semblables à ceux qui ont été récemment mis en évidence à la fois par des expériences de rhéo-optique et par des simulations numériques, observations qui sont en contradiction avec la théorie (classique) basée sur la rupture induite par l'écoulement de la mise en couches des particules (dans le domaine rhéofluidifiant). La dilatance résulte alors directement de l'acroissement de la FVE de la dispersion, étroitement associé à l'augmentation du volume de phase continue emprisonnée à l'intérieur des amas hydrodynamiques dont la taille croît avec le cisaillement. Les prédictions du modèle sont discutées en les comparant aux caractéristiques principales observées dans un grand nombre de dispersions dilatantes, spécialement les dépendences, en fonction de la fraction volumique, de la viscosité et des vitesses de cisaillement critiques (pour le seuil d'apparition de la dilatance, le maximum et la discontinuité de la viscosité), ainsi que les effets de la taille des particules, de la polydispersité et de la viscosité de la phase continue.

PACS. 82.70.-y Disperse systems – 83.20.Bg Macroscopic (phenomenological) theories – 83.50.Ax Steady shear flows – 83.50.Qm Thixotropy; thickening flows

[a] e-mail: quemada@lbhp.jussieu.fr
[b] CNRS ESA 7057

Introduction

The concept of effective volume fraction (EVF), previously re-visited [1] has been applied to structural modelling of the shear-thickening behavior of *weakly stabilized* dispersions in which shear induced flocculation (SIF) occurs [2]. The present article is devoted to similar modelling of shear-thickening "dilatant" behavior of *strongly stabilized* systems (herein called HS-systems), based on another process different from SIF, which obviously cannot be retained in this case as a possible explanation. Note that the term *stable* usually refers to systems which do not flocculate under quiescent (zero shear) conditions. In this series of papers, stable systems are further classified according to wether they flocculate or not under shear. The former are defined as *weakly stabilized* and the latter as *strongly stabilized*.

Numerous systems behave similarly to colloidal dispersions (insofar as the shear rate domain concerned is accessible to the measuring device), that is, shear thinning followed by shear thickening sometimes followed by shear thinning. More precisely, one observes shear thinning within a low shear rate region, $\dot{\gamma} < \dot{\gamma}_C$, followed by shear thickening up to a maximum at $\dot{\gamma} = \dot{\gamma}_M$ beyond which shear thinning occurs again. As the particle volume fraction ϕ is increased, the viscosity maximum at $\dot{\gamma}_M$ abruptly changes to a viscosity discontinuity (the corresponding shear rate will be here called $\dot{\gamma}_D$). Barnes [3] reviewed a large number of results from the literature, summing up the properties of parameters which generally control dilatancy characteristics, $\dot{\gamma}_C$, $\dot{\gamma}_M$ and $\dot{\gamma}_D$, especially their ϕ-dependences and the variation of the former with particle size ($\dot{\gamma}_C \propto a^{-2}$) and continuous phase viscosity ($\dot{\gamma}_C \propto \eta_F^{-1}$).

For a long time, disruption of shear-induced particle layering has been accepted as a possible explanation of shear thickening behavior. This Order-Disorder Transition (ODT) is based on the interpretation of early measurements by Hoffmann [4] carried out on electrostatically stabilized latex suspensions. For the first time, simultaneous rheological measurements and optical observations were associated, that clearly demonstrated the three domains of $\dot{\gamma}$ limited by the critical values, $\dot{\gamma}_C$ and $\dot{\gamma}_M$ (or $\dot{\gamma}_D$). Hoffmann interpreted these results by assuming that particle interactions and shear forces at low $\dot{\gamma}$ promote a progressive particle alignment in the flow direction. The resulting layers of 2D-packed spheres parallel to the rheometer plate, separated from one another by fluid layers, promote a lubricant effect, hence the observed shear thinning at low $\dot{\gamma}$. As $\dot{\gamma}$ grows, the relative velocity of adjacent layers increases, and so does the shear force exerted on the particles. At $\dot{\gamma} = \dot{\gamma}_C$, shear stress reaches a critical value at which particle layers are assumed to become unstable. Groups of spheres then leave their alignment and the resulting ODT leads to the viscosity increase, up to a maximum value at $\dot{\gamma} = \dot{\gamma}_M$. Note that for higher volume fractions, very rapid changes in diffraction patterns occur at $\dot{\gamma} = \dot{\gamma}_D$. Beyond $\dot{\gamma} = \dot{\gamma}_M$ (or $\dot{\gamma}_D$), an ordered flow resumes. The latter is related to the motion of single spheres, still distributed in layers in a hexagonal arrangement, however with individual rotation induced by the velocity gradient. Using a model based on DLVO theory of particle interactions, Hoffmann [5] calculated the shear rate at which the position of a doublet of particles in a layer becomes unstable under the total (hydrodynamic + DLVO) force, thus resulting in the viscosity increase. Although the model was not rigorously tested because of the limits of the approximations made throughout its development, it was able to predict the onset of instability.

More recently, in a simpler approach, Boersma and coworkers [6] derived $\dot{\gamma}_C$ from the balance of interparticle and shear forces between two single spheres of radius a. In the case of strong electrostatic stabilization and small interparticle (surface-to-surface) distance $h \ll a$, the model correctly predicts the effects of varying the particle size and the continuous phase viscosity, *i.e.* $\dot{\gamma}_C \propto \eta_F^{-1} a^{-2}$. The ϕ-dependence of $\dot{\gamma}_C$ was estimated by calculating $h(\phi)$ for different particle arrangements, however the resulting variation of $\dot{\gamma}_C(\phi)$ is not in agreement with the results collected by Barnes.

Many works have supported the layering hypothesis based on Hoffman's rheo-optical observations as an explanation of dilatancy. Numerical simulations ([7]), for example, which ignored hydrodynamic interactions, showed that particles lined up in files or layers parallel to the flow direction as the shear rate is increased.

On the other hand, several recent studies bring into question the validity of particle layering in HS-systems. Firstly, clustering effects were observed by Ackerson and Pusey [8] using light scattering measurements on sterically stabilized suspensions subjected to steady and oscillatory shear flows. Although their observations under oscillatory conditions appeared to be consistent with a sliding layer structure, scattering patterns observed under steady shear conflicted with the systematic presence of particle layering found in numerical simulations. These authors suggested the two following possible causes of failure of these simulations (*i*) absence of hydrodynamic interactions and (*ii*) particle ordering induced by the walls of the diffusion cell[1]. Moreover, Ackerson [9] pointed out that these light scattering experiments[2] do not demonstrate any strong ordering transition from the equilibrium liquid-like state. On the contrary, these observations rather demonstrated some evidence of particle ordering near cells boundaries.

Subsequent studies confirmed these findings. On the one hand, observations using neutron scattering and rheo-optical measurements [10–12] did not support the occurrence of particle layering but a shear induced clustering and showed that the onset of shear thickening is not necessarily due to ordering. The existence of clusters as transient structures was also introduced in a very recent work on dilatancy in sterically stabilized colloidal dispersions [13]. On the other hand, numerical simula-

[1] Note that this wall effect (likely the more probable explanation) could also be present in the rheometer gap and may have affected Hoffman's observations.

[2] Despite the fact that they were performed on samples with a volume fraction within a few percent of the freezing value, at shear rates well into the shear thinning transition.

tions based on Stokesian dynamics of HS-suspensions [14–16] showed that shear thickening results from the formation of transient "hydrodynamic clusters", not from an ODT. All these results have been corroborated by very recent rheo-optical measurements on sterically stabilized colloidal dispersions performed by Bender & Wagner [17]. They claimed that their results, interpreted through the colloidal stress-optical relationship [18], together with the results cited above, permit to "conclude that shear thickening consists of a process of forming hydroclusters regardless of whether a layered structure is present or not" [17].

Therefore, an ODT seems neither necessary nor sufficient for the observation of shear thickening behavior, thus leaving open to discussion the problem of identifying the mechanism responsible for this behavior in strongly stabilized dispersions.

Once the existence of such hydroclusters is admitted, it appears quite logical to tentatively apply to shear thickening the structural model developed in Part I, since this model is based on assuming the presence and the shear induced changes of structural units (SUs). This structural model is herein used, assuming a mechanism directly related to the hydrocluster formation. The proposed mechanism is a *shear induced change of the SU-compactness*, since hydroclustering necessarily promotes the imprisonment of suspending fluid between particles inside the cluster. This mechanism seems to be a plausible alternative to the ODT hypothesis[3].

The present work intends to show that such an hypothesis allows the structural model to predict the major part of the characteristics listed by Barnes, especially the ϕ-dependences of critical shear rates. As expected, the EVF concept introduced in Part I is the key to model's success since the EVF depends directly on both the number of particles entering the SUs and the SU-compactness.

The paper is organized as follows. Model assumptions are given (Sect. 1), then the model is developed (Sect. 2) and some of its predictions are presented (Sect. 3 and Sect. 4) and discussed (Sect. 5).

1 Assumptions of the model

As the shear rate is increased from zero, the following structural changes are assumed in the three domains $0 < \dot{\gamma} < \dot{\gamma}_1$, $\dot{\gamma}_1 < \dot{\gamma} < \dot{\gamma}_2$ and $\dot{\gamma}_2 < \dot{\gamma}$, dilatancy only appearing in the intermediate range of shear rate.

1. In the first domain, shear thinning is related to the progressive reduction of the SU-size as $\dot{\gamma}$ increases. However, as already discussed in Part I, HS-systems need a description different from that of partially flocculated systems. So, HS-systems will be here considered as a juxtaposition of large SUs. The latter are visualized as heterogeneous domains composed of dense sub-domains embedded in a loose medium. Sub-domains are seen as heterogeneous structures, similar[4] to the large SU to which they belong. Loose medium is seen as suspending fluid containing few particles. Analogous structures were recently assumed to exist in sterically stabilized dispersions, resulting from the "formation and breakup of large particle structures... that would not be aggregates in the normal sense, but simply mechanical locked arrays of particles with no long term stability" [13].
   Shear rate increase promotes a progressive separation of the denser parts of SUs (this process resembles SU-"rupturing" although it could also appear as a SU-"erosion"), these sub-domains thus forming new, smaller SUs. This reduction in SU-size is assumed to continue until a state is reached in which all SUs are changed into basic units. The latter are seen as small, compact clusters of primary particles[5] (herein called "compact-SUs"), within which primary particles are believed to have a large coordination number. On the contrary, each larger SU (in the shear thinning domain) can be seen as a group of compact-SUs, connected by either single or very small groups of primary particles, hence forming a small number of links between the compact-SUs.
2. At $\dot{\gamma} = \dot{\gamma}_1$, the progressive SU-breakup occuring in the first domain is supposed to stop at the level of basic SUs. Then, at the beginning of the second domain, $\dot{\gamma} > \dot{\gamma}_1$, the thinning-thickening transition is seen as resulting from a shear induced, progressive formation of clusters of basic-SUs. These clusters can be thought of as similar to the above-mentionned "hydrodynamic clusters" invoked in numerical simulations as "compact groups of particles formed when shear forces drive particles nearly into contact" [15], thus in close relation with short-range lubrication forces. Therefore, throughout the second domain, basic-SUs are assumed to progressively form groups of loose SUs, herein called "*hydroclusters*". Obviously, due to the immobilized volume of suspending fluid between particles inside the cluster, this structural change lowers the compactness φ of hydroclusters. The increase in EVF resulting from this φ-lowering leads to the viscosity raise.
3. Such a formation of an increasing number of hydroclusters continues until the onset of the third domain as a thickening-thinning transition is reached at an-

[3] The present work generalizes to "real" HS-systems (exhibiting successive shear thinning, shear thickening and shear thinning behavior as $\dot{\gamma}$ is increased) a previous structural modeling of "ideal" HS-systems, *i.e.* with "pure" shear thickening behavior [19].

[4] In model systems, fractal structures have been observed, involving their self-similarity at the different scales. In some extent (and very qualitatively) sub-domains within large SUs are seen as (self)-similar to these SUs.

[5] Such structures could be in part reminiscent of those formed during sample preparation. However, it is noteworthy that, depending on the system (nature of the particles, type of interactions, physiochemical characteristics...), complete rupturing of SUs could be reached at $= \dot{\gamma}_1$, *i.e.* basic-SUs could be the primary particles themselves : this case is also included in the model.

other critical shear rate, $\dot{\gamma} = \dot{\gamma}_2$, beyond which shear thinning is recovered by resuming a progressive erosion due to the "peeling off" of particles from hydroclusters. So, $\dot{\gamma}_2$ corresponds to the viscosity maximum reached as soon as all basic-SUs present at $\dot{\gamma}_1$ have formed hydroclusters, that is the case if the volume fraction is not high enough. On the contrary, the discontinuous viscosity will be accessible if the EVF reaches the maximum packing value (thus $\eta \to \infty$) before all of the basic-SUs have formed hydroclusters.

Obviously, the two critical shear rates, $\dot{\gamma}_1$ and $\dot{\gamma}_2$, should be identical to those which Barnes [3] introduced, $\dot{\gamma}_C$ and, either $\dot{\gamma}_M$ or $\dot{\gamma}_D$, respectively.

2 Model equations

The general expression (Part I, Eq. (2.8)) for the effective volume fraction of the suspension considered as a system composed of several populations characterized by (C_i, S_i) is given by:

$$\phi_{\text{eff}} = \left[1 + \sum_i C_i S_i\right] \phi. \tag{2.1}$$

This expression takes different forms in the three domains I, II and III, discussed in Section 1, as will be shown in the following.

2.1 In domain I

Shear thinning behavior[6] below $\dot{\gamma}_1$ is described as resulting from lowering the number fraction $\alpha(\dot{\gamma})$ of primary particles contained in the whole of SUs (both large and compact ones). Moreover, the progressive, shear-induced reduction of the mean SU-size is assumed to occur without significant change in the mean SU-compactness φ. This last assumption appears consistent with either breakup of large SUs or progressive, particle by particle, peeling off of smaller SUs. Moreover, in both cases, such changes are considered to occur without any significant rearrangement of their internal structure (the compactness of which could remain close to the Random Close Packing, for instance).

The shear dependence of α is supposed to be governed by relaxation kinetics, taking under steady conditions the same form as (Part I, Eq. (3.2))

$$\alpha = (\alpha_0 + \alpha_\infty \theta_a)\,(1 + \theta_a)^{-1} \tag{2.2}$$

with low and high shear limits α_0 and α_∞, and written in terms of the reduced shear rate, see (Part I, Eq. (3.4)), with a characteristic time t_a

$$\theta_a = (t_a \dot{\gamma})^p. \tag{2.3}$$

[6] Obviously, the model also works in the absence of this first decrease in viscosity, assuming the SU-structure remains unchanged up to $\dot{\gamma}_1$.

2.2 In domain II

Between $\dot{\gamma}_1$ and $\dot{\gamma}_2$, a quantitative description of dilatancy results from the assumption made in Section 1, *i.e.* without further SU-breakup, with structure rearrangement only. This assumption requires that the total number of particles involved in all the SUs should not decrease beyond $\dot{\gamma}_1$, hence the fraction of particles involved in all the SUs should remain constant over the whole domain II, thus equal to its value at the onset of shear thickening,

$$\alpha_1 \equiv \alpha(\dot{\gamma}_1).$$

In this domain, the model thus supposes the *coexistence* of two populations, basic-SUs and hydroclusters, with α and β being the number fractions of primary particles contained in all the SUs of each kind, respectively. Moreover, as $\dot{\gamma}$ increases, the number of particles involved in hydroclusters, starting from zero at $\dot{\gamma} = \dot{\gamma}_1$, raises at the expense of α_1, which requires the condition, $\alpha(\dot{\gamma}) + \beta(\dot{\gamma}) = \alpha_1$.

The shear dependence of β is supposed (again for simplicity) to be still governed by relaxation kinetics, *i.e.* still of the same form as (Part I, Eq. (3.2)), but taking the required limiting condition $\beta(\dot{\gamma}_1) = 0$ into account. Using the reduced shear rate and its critical value,

$$\theta_b = (t_b \dot{\gamma})^q \text{ and } \theta_{b1} = (t_b \dot{\gamma}_1)^q$$

$\beta(\dot{\gamma})$ is thus given by

$$\beta = \beta_\infty (\theta_b - \theta_{b1})(1 + \theta_b)^{-1}. \tag{2.4}$$

2.3 In domain III

For $\dot{\gamma} > \dot{\gamma}_2$, the model is more imprecise. At $\dot{\gamma} = \dot{\gamma}_2$, shear forces are supposed to be capable of restarting first the breakup of hydroclusters. However, a question remains open: what kind of SUs will be formed beyond $\dot{\gamma}_2$? Though formation of basic-SUs seems the more probable, the large shear force (especially in the case of discontinuous viscosity) could promote the formation of smaller SUs, such as broken basic-SUs or primary particles[7]. For generality, it is thus assumed that beyond $\dot{\gamma}_2$ hydroclusters progressively form new SUs at the expense of β, with a number fraction $\beta'(\dot{\gamma}) = \beta_2 - \beta(\dot{\gamma})$, where $\beta_2 \equiv \beta(\dot{\gamma}_2)$. Hence, β decreases from β_2 and β' increases from 0 whereas α remains fixed at the value $\alpha_2 \equiv \alpha(\dot{\gamma}_2) = \alpha_1 - \beta_2$.

[7] Such cases can be directly included in the same calculation, by just changing the φ_S of new SUs to either φ_a (for compact-SUs) or $\varphi_S = 1$ for single particles. Note that, as discussed later in the paper, this choice does not critically influence the model's predictions. Moreover, in all cases, it is assumed that the resumption of shear thinning just beyond $\dot{\gamma}_2$ is related to the reduction of hydroclusters prior to that of compact-SUs, the former being considered as more fragile than the latter. (Such a process could be possibly followed by disruption of the latter at higher shear rates).

The shear dependence of β' is again supposed to be governed by relaxation kinetics, with a form similar to (2.4),

$$\beta'(\dot\gamma) = \beta_\infty(\theta_s - \theta_{s2})(1+\theta_s)^{-1} \tag{2.5}$$

now taking the required limiting condition $\beta'(\dot\gamma_2) - 0$ into account and using the reduced shear rate and its critical value,

$$\theta_s = (t_s\dot\gamma)^r \quad \text{and} \quad \theta_{s2} = (t_s\dot\gamma_2)^r.$$

Summarizing, the model is based on the following relations giving the number fractions of the assumed three populations of SUs, α , β and β', hence the corresponding values of ϕ_{eff} (2.1):

- For $0 \le \dot\gamma \le \dot\gamma_1$,

$$\alpha = \alpha(\dot\gamma) \quad \text{and} \quad \beta = 0 \tag{2.6}$$

$$\phi_{\text{eff}} = [1 + C_a\alpha]\phi. \tag{2.7}$$

- For $\dot\gamma_1 \le \dot\gamma \le \dot\gamma_2$,

$$\alpha = \alpha(\dot\gamma) = \alpha_1 - \beta \quad \text{where} \quad \alpha_1 = \alpha(\dot\gamma_1) \tag{2.8}$$

$$\beta = \beta(\dot\gamma) \quad \text{with} \quad \beta(\dot\gamma_1) = 0$$

$$\phi_{\text{eff}} = [1 + C_a\alpha_1 + (C_b - C_a)\beta]\phi. \tag{2.9}$$

- For $\dot\gamma_2 \le \dot\gamma$,

$$\alpha = \alpha_1 - \beta_2 \quad \text{where} \quad \beta_2 = \beta(\dot\gamma_2) \tag{2.10}$$

$$\beta = \beta(\dot\gamma) = \beta_2 - \beta'$$

$$\beta' = \beta'(\dot\gamma) \quad \text{with} \quad \beta'(\dot\gamma_2) = 0$$

$$\phi_{\text{eff}} = [1 + C_a\alpha_1 + (C_b - C_a)\beta_2 + (C_s - C_b)\beta']\phi. \tag{2.11}$$

In equations (2.7, 2.9) and (2.11), the compactness factors C_a , C_b and C_s are related to φ_a , φ_b and φ_s , respectively through (Part I, Eq. (2.7))

$$C_i = \varphi_i^{-1} - 1 \qquad (i = a, b, s).$$

Standard values of φ_i can be chosen:

- for SU-compactness at low shear rate, the Random Close Packing $\varphi_a = \varphi_{RCP} = 0.637$;
- for hydroclusters, a "composite" packing, $\varphi_b = 0.74 \times 0.71 = 0.525$, resulting from compact-SUs (with $\varphi_{FCC} = 0.74$, the FCC packing of single monodisperse spheres) packed at the hard sphere maximum packing at high shear ($\varphi = 0.71$) [20];
- for the third population, a value between $\varphi_s = 1$ (in the case of single particles formed by peeling off) and $\varphi_s = \varphi_{FCC}$ (for compact-SUs). Nevertheless, as the φ_s-value was found to have only a slight influence on the results, the choice $\varphi_s = \varphi_a$ was simply taken to test the predictions of the model.

Before predicting the variation of $\eta(\dot\gamma)$ at different volume fractions as Hoffmann observed [4], the dilatancy region, $\dot\gamma_1 \le \dot\gamma \le \dot\gamma_2$, will be studied in more detail as a first test of the model. Specifically, one has to check that the two boundaries of this region exhibit the same features as the limiting values $\dot\gamma_C$ and $\dot\gamma_M$ (or $\dot\gamma_D$) observed by many researchers and that Barnes listed and discussed in his review. In the next section, it will be shown that the simple assumption of "local dilatancy" (in the sense of progressive formation of looser SUs beyond the onset of dilatancy), in association with the EVF concept, automatically leads to these features.

3 Prediction of critical shear rates as a preliminary test of the model

3.1 Critical shear rate $\dot\gamma_D$ (for discontinuous viscosity)

The simplest test consists of checking that the model predicts the viscosity discontinuities that Hoffmann observed at a volume fraction between about 0.5 and 0.6. With the present model, based on the $\eta(\phi)$, (see Part I, Eq. (2.3)),

$$\eta_r = (1 - \frac{\phi_{\text{eff}}}{\phi_m})^{-2}$$

such discontinuities are obtained as soon as ϕ_{eff} reaches the maximum packing ϕ_m, that thus defines the shear rate at the discontinuity, $\dot\gamma_2 = \dot\gamma_D$. Putting $\phi_{\text{eff}} = \phi_m$ in (2.9) gives an equation for β, the solution of which is β_D . Written from (2.4) in terms of $\theta_{bD} = (t_b\dot\gamma_D)^q$, this solution is thus defined by

$$\frac{\phi_m - A\phi}{B\phi} = \frac{\theta_{bD} - \theta_{b1}}{1 + \theta_{bD}} \tag{3.1}$$

where $A = (1 + C_a\alpha_1)$ and $B = \beta_\infty(C_b - C_a)$. Solving equation (3.1) in θ_{bD} leads to an expression for $\dot\gamma_D$ in the following form

$$\dot\gamma_D = t_b^{-1}\left[\frac{1 - \dfrac{\phi}{\phi_{m2}}}{\dfrac{\phi}{\phi_{m1}} - 1}\right]^{\frac{1}{q}} \tag{3.2}$$

introducing the two effective packings ϕ_{m1} and ϕ_{m2}

$$\phi_{m1} = \frac{\phi_m}{A + B} \tag{3.3a}$$

$$\phi_{m2} = \frac{\phi_m}{A - B(t_b\dot\gamma_1)^q}\,. \tag{3.3b}$$

Both depend on $\dot{\gamma}_1$, through θ_{b1} and

$$\alpha_1 = (\alpha_0 + \alpha_\infty \theta_{\alpha 1})\,(1 + \theta_{\alpha 1})^{-1} \text{ with } \theta_{\alpha 1} = (t_a \dot{\gamma}_1)^p \tag{3.4}$$

from (2.3) and (2.2), respectively.

These two effective packings limit the ϕ-domain where the viscosity may diverge: clearly, (3.2) gives positive values of $\dot{\gamma}_D$ only if $\phi_{m1} < \phi < \phi_{m2}$, that is if ϕ lies within a limited range, as was observed experimentally. It is noteworthy that this result has been obtained from the sole assumption of the existence of two populations: basic-SUs and hydroclusters, and using the EVF in a viscosity relation $\eta(\phi)$. Neither the precise form of the latter (provided that it contains explicitly a maximum packing ϕ_m) nor the precise form of shear rate dependences (provided that the structure kinetics are of the relaxation type) are required to get this limited ϕ-range for diverging viscosity[8].

3.2 Critical shear rate $\dot{\gamma}_1$ at the onset of dilatancy

Since $\dot{\gamma}_1$ appears in (3.3), further improvement of the model requires definition of this value.

Barnes' compilation showed an inverse quadratic dependence on particle size (over several decades in particle size, see [3], Fig. 5). It is worth noting that this finding roughly corresponds to a *constant* hydrodynamic force exerted on a primary particle at the onset of dilatancy, $\approx \eta_{\text{eff}} \dot{\gamma}_C\, a^2$, where η_{eff} is an effective viscosity of the fluid.

From the empirical result, $\dot{\gamma}_C \approx a^{-2}$, one thus assumes that formation of hydroclusters from basic-SUs occurs as soon as the hydrodynamic force *per particle* $f_H \approx \eta_{\text{eff}} \dot{\gamma}\, a^2$ is larger than a critical value f_C. Taking $\eta_{\text{eff}} = \eta(\phi, \dot{\gamma})$, the dispersion viscosity (in order to take hydrodynamic interactions at high volume fraction into account), this condition $f_H \geq f_C$ defines the onset of dilatancy $\dot{\gamma}_1$ as the solution of the equation

$$\eta(\phi, \dot{\gamma}_1)\, \dot{\gamma}_1 = f_c / a^2 \tag{3.5}$$

where

$$\eta(\phi, \dot{\gamma}_1) = \eta_F \left[1 - \frac{\phi}{\phi_m}(1 + C_a \alpha_1)\right]^{-2}$$

is the viscosity of the suspension at the onset of dilatancy. Hence (3.5) gives both the volume fraction and particle radius dependences $\dot{\gamma}_1(\phi, a)$.

From (3.5), it appears that the onset of dilatancy is governed by a critical shear stress (per particle) $\sigma_C = f_C / a^2$, not a critical shear rate, in agreement with a large number of investigations (see below, Sect. (5.4)). Moreover, the product $w_C \approx f_C a$ scales the hydrodynamic energy (per particle) required for hydroclustering, and thus enters the critical ratio (which works as a critical Péclet number)

$$\frac{w_C}{KT} \approx \frac{\sigma_C\, a^3}{KT} = Pe_C$$

which will be herein taken as an open parameter of the model.

Obviously, Barnes' data is bounded by two curves $\dot{\gamma}_1 \propto (2a)^{-2}$ as solutions of (3.5) for two different values of f_C , at given volume fraction ϕ. These curves were found to be very close to straight lines, except at very high ϕ approaching the maximum packing. For $\phi \simeq 0.5$, the limiting f_C-values are found about 0.5×10^{-12} N and 50×10^{-12} N. The intermediate value[9] corresponds to a reduced critical energy per particle close to $w_C/KT \cong 120$ for particles of radius $a - 0.1$ μm.

Note that these limiting values are not strongly dependent on ϕ, except close to ϕ_m. This is shown from Barnes' data with f_C-values (in 10^{-12} N unit) such as $0.1 < f_C < 20$ at $\phi = 0.3$ and $2 < f_C < 200$ at $\phi = 0.6$. In fact, f_C essentially depends on ϕ through the high shear limit of the shear thinning viscosity: in (3.5), for particle size > 0.1 μm (that is the case of almost all compiled studies), $\theta_{a1} \approx Pe_C \approx 10^2$. This value is large enough to make $\alpha_1 \cong \alpha_\infty$, so to give directly $\dot{\gamma}_1 = f_C / \eta(\phi, \infty) a^2$, so $f_C \propto \eta(\phi, \infty)$.

From the solution $\dot{\gamma}_1(\phi)$ of (3.5) for a given radius a , it is now possible to determine the two limiting packings ϕ_{m1} and ϕ_{m2}, and hence to describe the variations of $\dot{\gamma}_D$ and $\dot{\gamma}_C \equiv \dot{\gamma}_1$, as functions of ϕ .

3.3 Critical shear rates $\dot{\gamma}_D$ and $\dot{\gamma}_C$ as functions of volume fraction

Model predictions were tested on a dispersion of spherical particles of radius $a = 0.1$ μm, taking the following values for the model variables:

- for basic-SUs $\{t_a = 5$ ms $(\cong t_{Br}),\ p = 0.5\}$;
- for hydroclusters $\{t_b = 20$ ms, $q = 1\}$;
- for reduced hydroclusters, $\{t_s, r\} \equiv \{t_a, p\}$ for the sake of simplicity.

Figure 1 shows typical variations of $\dot{\gamma}_C$ and $\dot{\gamma}_D$ *vs.* ϕ, for three critical values of the dimensionless ratio $Pe_C = w_C/KT$: 10, 50, 100. Note that these variations exhibit the main features that Barnes described (see Fig. 2 and 3 in reference [3]), in particular:

(i) $\dot{\gamma}_C$ and $\dot{\gamma}_D$ tend to zero around the maximum packing fraction ϕ_{m2} (close to ϕ_m);

(ii) $\dot{\gamma}_C$ begins to increase very rapidly (just below ϕ_{m2}) and slower and slower as ϕ decreases, tending to a finite value at low ϕ. Although this variation seems to contradict the general behavior (a divergence in $\dot{\gamma}_C$ as $\phi \to 0$) displayed in [3], Figure 3, one may observe however that other works exhibit a finite limit, as shown in [3], Figure 2, noticeably those of Wagstaff and Chaffey [21], Hoffman [4,5] and maybe also some other data, but this is not certain owing to the absence of measurements in the low ϕ-range;

[8] On the contrary, the precise values of ϕ_{m1} and ϕ_{m2} clearly depend on the details of the kinetics.

[9] This value $f_C = 5 \times 10^{-12}$ N, corresponds to a reduced value of critical energy per particle close to $w_C/KT \cong 1200\ a_{\mu\text{m}}$, where $a_{\mu\text{m}}$ is the value of the particle radius expressed in microns.

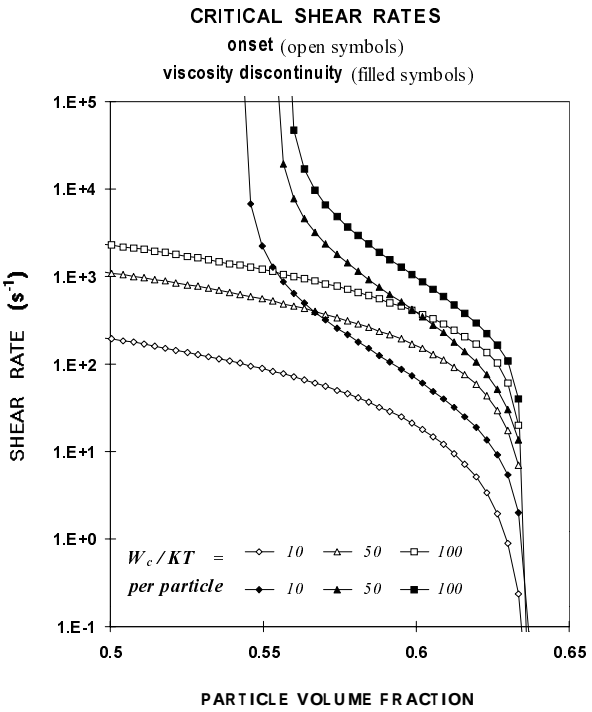

Fig. 1. Critical shear rates $\dot{\gamma}_c$ and $\dot{\gamma}_D$ *vs.* volume fraction ϕ for three values of w_c/KT per particle = 10, 50, 100 (σ_c-values: 3 , 15 , 30 Pa) spherical particles (radius $a = 0.1$ μm) dispersed in a Newtonian fluid (viscosity $\eta_F = 1$ mPa.s). Model variables: $\phi_M = 1$, compact-SUs: $\varphi_a = 0.637$; $\alpha_0 = 1$ and $\alpha_\infty = 0.72$ [10]; $\{t_a, p\} = \{5$ ms, $0.5\}$, hydroclusters: $\varphi_b = 0.525$; $\beta_\infty = 1$; $\{t_b, q\} = \{20$ ms, $1\}$, reduced hydroclusters: $\varphi_s \equiv \varphi_a = 0.637$; $\{t_s, r\} \equiv \{t_a, p\}$.

(iii) $\dot{\gamma}_D$ (*i.e.* in the case $\phi_{m1} < \phi < \phi_{m2}$) shows the same behavior as $\dot{\gamma}_C$ just below ϕ_{m2} and diverges at $\phi = \phi_{m1}$ as ϕ decreases, in qualitative agreement with Barnes'data (cf. [3], Fig. 4).
Lastly, note that raising Pe_C leads to a general increase in both $\dot{\gamma}_C$ and $\dot{\gamma}_D$, and to a reduction of the ϕ-interval between $\dot{\gamma}_C$ and $\dot{\gamma}_D$.

3.4 Critical shear rate $\dot{\gamma}_M$ at the maximum of dilatancy (case when $\phi < \phi_{m1}$)

For $\phi < \phi_{m1}$, the viscosity discontinuity disappears ($\dot{\gamma}_D$ does not exist) and is replaced by a viscosity maximum at a new critical shear rate value, $\dot{\gamma}_2 \equiv \dot{\gamma}_M$, above which shear thinning reappears. This maximum should occur whenever all the basic-SUs present at $\dot{\gamma}_1$ have been changed into hydroclusters without reaching the value $\phi_{\text{eff}} = \phi_m$ at which the viscosity diverges. Since β increases at the expense of α_1 , the viscosity maximum at

[10] these α-values result from equation (1.14) with α_0 and α_∞ in place of S_0 and S_∞, applied to hard sphere dispersions which exhibit limiting maximum packings $\phi_0 = 0.63$ and $\phi_\infty = 0.71$ (de Kruif *et al.*, 1985).

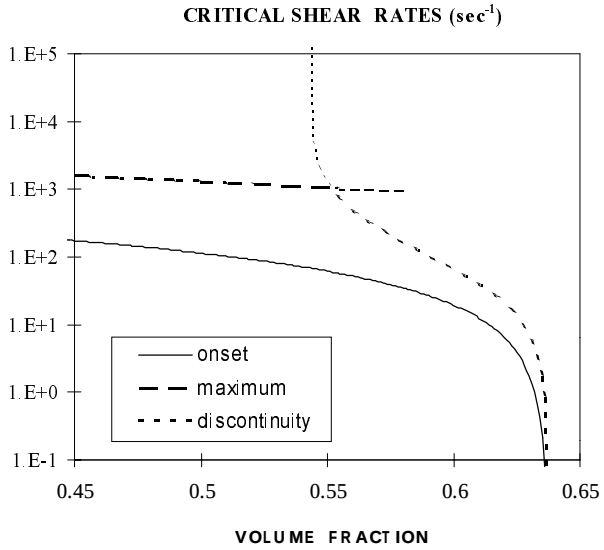

Fig. 2. Critical shear rates $\dot{\gamma}_c$, $\dot{\gamma}_D$ and $\dot{\gamma}_M$ *vs.* volume fraction ϕ, for $\sigma_c = 1$ Pa (corresponding value: $w_c \approx 3KT$, for particle radius $a = 0.1$ μm) (same values of model variables as in Fig. 1).

$\dot{\gamma} = \dot{\gamma}_2$ will occur when $\beta_2 = \alpha_1$. Using (2.8), one obtains

$$\alpha_2 \equiv \alpha(\dot{\gamma}_2) = \alpha_1 - \beta_2 = 0$$

that defines $\dot{\gamma}_2$ as a function of $\dot{\gamma}_1$ (through θ_{b1} and α_1), thus giving $\dot{\gamma}_M = \dot{\gamma}_2$ *vs.* ϕ,

$$\dot{\gamma}_M = t_b^{-1} \left[\frac{\beta_\infty \theta_{b1} + \alpha_1}{\beta_\infty - \alpha_1} \right]^{\frac{1}{q}} . \qquad (3.6)$$

Figure 2 shows the variation of $\dot{\gamma}_C$, $\dot{\gamma}_D$ and $\dot{\gamma}_M$ *vs.* ϕ , for the same model parameter values used in Figure 1, and taking $w_C/KT \cong 3$. These variations are in rather good agreement with measurements recently performed by Keller & Keller, Jr [22] on coal-water dispersions which clearly showed differences between $\dot{\gamma}_D$ and $\dot{\gamma}_M$ (see [22], Fig.3). Although the present model, using another set of model variables, succeeds in predicting Keller's curves, both in order of magnitude and shapes, the comparison is not discussed further here since, at this stage, the values of model variables remain very empirical, and so difficult to interpret, owing to the complex nature of coal-water dispersions.

4 Some other predictions of the model

4.1 Rheograms $\eta = \eta(\dot{\gamma})$ at different volume fractions

Figure 3 shows several rheograms, $\eta(\dot{\gamma})$, calculated at different volume fractions, for $a = 0.1$ μm and $f_C = 0.5 \times 10^{-12}$ N (*i.e.* $w_C/KT \cong 12$), taking the values already used in Figure 1 for the other variables. The main features of these rheograms are very similar to Hoffman's results [4]. The minimum ϕ-value above which the viscosity discontinuity appears is found close to $\phi_{m1} = 0.53$. This

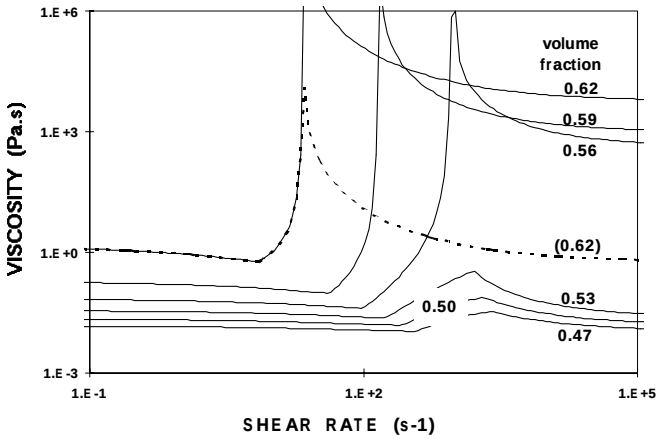

Fig. 3. Model rheograms, η *vs.* $\dot{\gamma}$, calculated at different volume fractions, which exhibit same type of viscosity discontinuities as those Hoffman observed. Model variables: $\phi_M = 1$, compact-SUs: $\varphi_a = 0.637$; $\alpha_o = 1$; $\alpha_\infty = 0.72$; $\{t_a, p\} = \{0.6$ ms, $0.5\}$, hydroclusters: $\varphi_b = 0.525$; $\beta_\infty = 1$; $\{t_b, q\} = \{20$ ms, $1\}$, reduced hydroclusters: $\varphi_s = 0.637$; $\{t_s, r\} = \{t_a, p\}$.

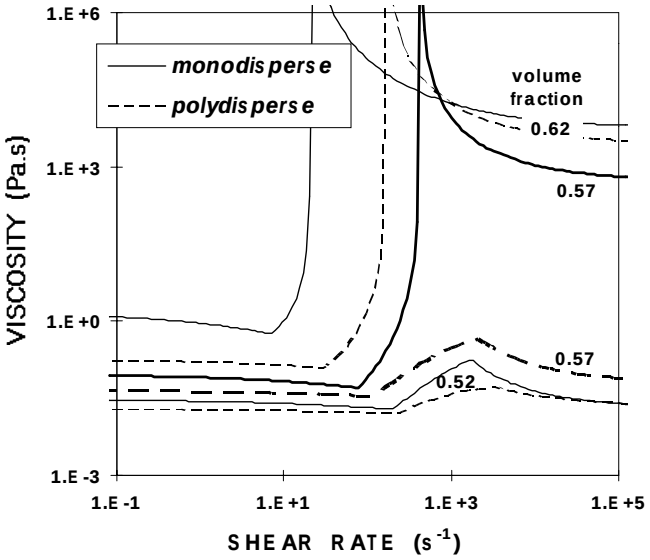

Fig. 4. Effect of polydispersity on model rheograms, η *vs.* $\dot{\gamma}$ for two compactness values: monodisperse particles $(\varphi_a; \varphi_b) = (0.637; 0.525)$, polydisperse particles $(\varphi_a; \varphi_b) = (0.67; 0.58)$ (remaining model variables : same values as in Fig. 3).

result is directly related to the compactness $\varphi_b = 0.525$ assumed for hydroclusters: as $\alpha_0 \leq \alpha_1 \leq \alpha_\infty$, ϕ_{m1} is found in the range $0.525 \leq \phi_{m1} \leq 0.574$. The fact that a similar value was found in Hoffman's study may be considered as supporting the assumption of (loose) hydroclusters. Note that changing the ratio w_C/KT, modifies the α_1-value given by (3.4), and hence the values of ϕ_{m1} and ϕ_{m2}.

As clearly shown within the third domain $\dot{\gamma} > \dot{\gamma}_D$, if $\phi > \phi_{m1}$, the viscosity decrease beyond the discontinuity is not correctly described, as is shown in Figure 3 by the dashed curve drawn for $\phi = 0.62$. This discrepancy probably results from the crudeness of the model in this region $\dot{\gamma} > \dot{\gamma}_D$: assuming the same values for the pairs $\{t_s, r\}$ and $\{t_a, p\}$, *i.e.* identical kinetics for basic-SUs and reduced hydroclusters seems very questionable. However, since the dispersion viscosity diverges at $\dot{\gamma} = \dot{\gamma}_D$, one may postulate that, just beyond $\dot{\gamma}_D$, the system should exhibit plastic-like behavior. Within the rheometer gap, close to the rotating wall, this could be seen as leading to the formation of a thin fluid layer in which the shear stress is high enough to induce the breakdown of hydroclusters. The presence of such a "lubricant" layer has been roughly taken into account by assuming that shear forces can effectively break up only a very small fraction of hydroclusters available at $\dot{\gamma} = \dot{\gamma}_D$, *i.e.* by multiplying the variable β' in (2.5) by a factor $\xi \ll 1$. In practice, beyond $\dot{\gamma}_D$, the viscosity curves shown in Figures 3, 4 and 5 were calculated arbitrarily taking $\xi = 0.01$ for $\phi > \phi_{m1}$ whilst keeping $\xi = 1$ for $\phi < \phi_{m1}$. The resulting description, although qualitatively better, still remains unsatisfactory. This indicates that a more precise description of the structure in the domain beyond $\dot{\gamma}_D$ will be needed for future improvement of the model.

4.2 Effect of particle polydispersity

Explaining dilatancy as resulting from the breakup of well-ordered layers of particles is certainly questionable in the case of complex fluids, for which broad distributions of individual particles in both size and shape are usually observed. Nevertheless, as clustering also occurs in such polydisperse fluids, it seems possible to built a very similar structural model after changing some parameters, in particular using new values for the compactnesses φ_a and φ_b. As polydispersity obviously should increase the compactness of any SU (more especially that of the hydrocluster) in comparison with those chosen for monodisperse systems, it should be more difficult to observe dilatancy in complex fluids. Moreover, another cause of decreased dilatancy might be the reduction of the difference $(\varphi_a - \varphi_b)$ which reduces the interval $(\phi_{m2} - \phi_{m1})$, blurring the viscosity discontinuity.

Figure 4 shows how the predictions of the model are changed after modifying φ_b, whilst keeping unchanged

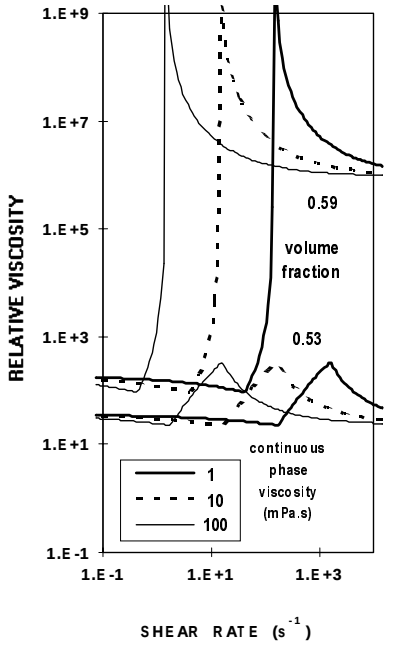

(a)

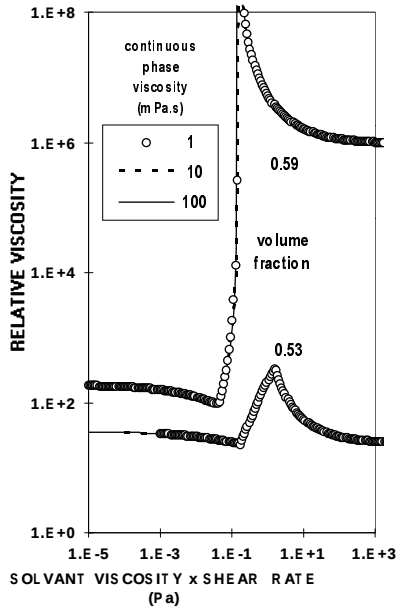

(b)

Fig. 5. Effect of the continuous phase viscosity on model rheograms, η *vs.* $\dot{\gamma}$. Relative viscosity η_R at $\phi = 0.59$ and $\phi = 0.53$ (same values of model variables as in Fig. 3). (a) Curves $\eta_R = f(\dot{\gamma})$, for $\eta_F = 1$, 10, 100 mPa.s. (b) Reducing curves of Figure 5a into a master curve $\eta_R = f(\eta_F\dot{\gamma})$.

the previously used model variables, excepted the value $\varphi_b = 0.525$ which was replaced by $\varphi_b = 0.58$. Note that for φ-values roughly centered in the interval (ϕ_{m1}, ϕ_{m2}), the discontinuity in viscosity disappears and changes to a maximum if φ_b is increased, see Figure 4, the intermediate rheogram, for $\phi = 0.57$. Quite similar features were obtained using different φ_b-values, provided that they are higher than those used for monodisperse suspensions.

4.3 Effect of the continuous phase viscosity

As Barnes [3] pointed out, changing the viscosity of the continuous phase, η_F, modifies dilatancy. The most obvious effect results from the direct proportionality of the dispersion viscosity on η_F, which implies that the relative viscosity, η_R, must be used to evaluate the actual role of η_F.

A large number of studies (see Refs in [3]) showed that dilatancy can be dispaced to higher shear rates by lowering η_F. This has been confirmed in Boersma *et al.*'s work [6] in which lowering η_F by heating from 20 to 50 ℃ increases the shear rate for the onset of dilatancy by more than one decade. The present model predicts similar features of the relative viscosity as shown in Figure 5a, taking $\eta_F = 1$, 10, 100 mPa s. for two volume fractions, below and above ϕ_{m1}, respectively. As expected, these three curves collapse onto a master curve, Figure 5b, if the product of the continuous phase viscosity and the shear rate is used as the variable.

5 Discussion

5.1 Particle layering and change in cluster compactness due to hydrocluster formation

As the basic assumption used in the present model is the shear induced change in SU-compactness, it should be discussed in comparison with the ODT assumption (that is the disruption of particle layering promoted by shear) used in other models.

For HS-systems, the presence of transient clusters in the shear rate range around the onset of dilatancy — that seems now well-established from both rheo-optical experiments and numerical simulations — seems to be the most convincing argument against ODT. However, once the presence of clusters is accepted, the nature of these clusters and the mechanism leading to the onset of dilatancy remains open to discussion.

Though supported by many simulations and rheo-optical observations [10–17], the presence of a layered structure to explain shear-thinning at low shear is questionable. This is due to several reasons since such a presence (*i*) should impede cluster formation, (*ii*) is rather improbable in highly polydisperse systems exhibiting dilatancy, (*iii*) might be related to wall-induced ordering (both in simulations and experiments). Alternatively, for $\dot{\gamma} < \dot{\gamma}_C$, shear-thinning has been herein related to a progressive reduction of initially large, loose clusters (more probably clusters of clusters) of compact-SUs, as the basic-SUs[11]. In a similar way, general assumptions for inter-

[11] remembering that, if the volume fraction is high enough, such basic-SUs have been assumed to pre-exist (probably not independently from sample preparation) as SUs formed of close packed primary particles.

preting shear-thinning in numerous complex fluids, shear-thinning prior to thickening in dilatant systems is believed to result from the release of an increasing volume of the fluid immobilized inside the SUs whose size decreases as the shear rate increases.

At $\dot{\gamma} = \dot{\gamma}_C$, a new process starts to change progressively the structure of the system, now considered as a suspension of basic-SUs. Two processes can be postulated to explain dilatancy beyond $\dot{\gamma}_C$: (a) the (herein used) formation of hydroclusters — as soon as hydrodynamic force overcome the mean Brownian force [17] —; (b) a shear induced change in the compactness of basic-SUs, leading to a kind of "local dilatancy", already proposed in a previous work [23]. These two processes can be discussed and compared as follows:

(a) The formation of hydroclusters seems the best established process to explain dilatancy beyond $\dot{\gamma}_C$: in the framework of the present model, the viscosity enhancement directly results from raising the amount of continuous phase imprisoned in clusters whose size increases as $\dot{\gamma}$ grows, whatever the shape of the cluster is. However, from numerical simulations in Hard Sphere systems [15] hydroclustering is found to be highly sensitive to Brownian motion. Actually, inclusion of a very small amount of Pe^{-1} ($\approx 10^{-4}$) efficiently destroys the larger clusters, thus eliminating "hydrodynamic" dilatancy if Pe does not reach high enough values[12], which must be even higher in the case of a soft repulsive potential. Such a high sensitivity to the Péclet number might render this type of clustering questionable in the case of many HS-suspensions of colloidal size.

(b) The second process is a shear induced SU-deformation which necessarily involves relative particle displacement inside the SU, thus changing the SU-compactness. It is thus assumed that at $\dot{\gamma} = \dot{\gamma}_C$ shear forces become capable of promoting only a relative displacement of particles inside the SU. This means that shear forces are there only able to overcome some cohesive forces inside the compact-SU, not to break it. As a consequence, beyond $\dot{\gamma}_C$, compact-SUs are progressively changed into loose SUs, here called "*dilated-SUs*". The resulting EVF increase from this decreased compactness necessarily raises the viscosity. Although no direct proof was given of the existence of such a structural change in SUs at the onset of dilatancy, it is noteworthy that, as a kind of "local dilatancy", this assumption appears in complete agreement with the classical concept of dilatancy described very early by Reynolds [24]. Note that such a concept requires an initial volume expansion, demonstrated by the often observed drying out of the free surface of the sample (as observed in coarse granulo-viscous media for instance [27]). However, as such a "local dilatancy" assumption is still rather speculative, further work is required, *e.g.* some confirmation from rheo-optical measurements.

[12] for instance, $Pe > 10^2 - 10^3$ for an area fraction ≈ 0.45.

Nevertheless, it is worth emphasizing the complete similarity in the model equations corresponding to these two processes (a) and (b), independent of whether the presence of hydroclusters or dilated-SUs is assumed. In particular, the compactness φ_b and kinetic variables corresponding to these two kinds of SUs are involved in the same way. Hence, the choice of process (a) or (b) will only influence the interpretation of the model variables, not the model's predictions using given values of the latter.

Note that in Frith *et al.*'s work on dilatancy in colloidal dispersions [13], clusters were also introduced as transient structures. However, two different types of structural changes (which were not well defined in the paper) were assumed in order to explain the observed rheological behavior, depending on ϕ: (i) a gradual structural change which leads to shear thickening (with a finite maximum in viscosity), at low volume fraction, and (ii) some micro-structural transition related to the discontinuous dilatancy (with a diverging viscosity), at higher volume fraction. It is noteworthy that, on the contrary, the *same microstructural process* is introduced in the present model, whatever the volume fraction is. This unique structural process seems to offer a simpler framework for describing dilatancy.

Finally, caution is required in classifying the system. Is it a "strongly stabilized" system or a system in which shear stresses can overcome the (more or less moderate) repulsive forces (herein called HS-system and PF-system, respectively)? In the latter case, shear thickening will result from particle capture and lead to formation of a floc, thus increasing the EVF, and hence the viscosity: the model to be used is the Shear Induced Flocculation model [2], in which thickening originates from the type of shear-dependence of kinetic constants. On the contrary, in the former case, the source of thickening is quite different: the formation of hydroclusters — which involves hydrodynamic and Brownian forces only — as new structural units with their proper kinetics.

5.2 Particle size effects

Analyzing the effect of particle size on the critical shear rates requires some attention. The present work uses the empirical result (from Barnes' review) $\dot{\gamma}_C \approx a^{-2}$ considered as a validation of the assumption that the onset of dilatancy is reached as soon as the hydrodynamic force on a primary particle (which scales as $\eta_{\text{eff}}\dot{\gamma}a^2$) is larger than a critical value. In pure HS-systems, the latter should result from repulsive Brownian interactions. However, in stable colloidal dispersions, this critical value could be seen as reflecting the expected role played by the interaction potential at the level of individual particles[13]. It is worthy of note that the mean value of f_C needed to fit Barnes' data has a magnitude $f_C \approx 10^{-12}$ N in agreement with

[13] More precisely, the second derivative of the total potential created by neighbouring particles within the compact-SU (like in a colloidal gel).

standard values of the force of interaction in colloidal dispersions with particle radius $a \approx 0.1 - 1\ \mu$m [25].

On the other hand, $\dot{\gamma}_D$ at the viscosity discontinuity could depend on the particle radius in a more complex manner, due to the (size-dependent) interaction potential $W_I(a)$, see Part I, equation (3.2), with t_b varying as $\eta_{\rm eff} a^3/W_I(a)$, see Part I, equation (3.5)[14]. In the case of soft colloidal spheres, the interaction potential results from superimposing electrostatic repulsion and van der Waals attraction, which are both proportional to the sphere radius a , thus leading to $\dot{\gamma}_D \propto a^{-2}$. On the contrary, steric repulsion which depends strongly on polymer characteristics and solvent quality is generally independent of a, thus leading to $\dot{\gamma}_D \propto a^{-3}$ in sterically stabilized dispersions (though special cases with $W_I(a) \propto a$ can be found [26] then still giving $\dot{\gamma}_D \propto a^{-2}$).

In their work on sterically stabilized suspensions [13] — performed in several media with different solvency and viscosity, corresponding to hard and soft repulsions — Frith and co-workers reported a $\dot{\gamma}_D$-dependence in a^{-3} for hard sphere systems and rather in a^{-2} for softer systems, which is in agreement with the above discussion. However, partly due to the use of stress controlled rheometers, the onset of dilatancy was not defined in the same manner as in the present work. In fact, these authors retained two definitions depending on whether the volume fraction is high or low. They chose either the abrupt change in viscosity following the shear thinning in the first case thus making this onset the same as $\dot{\gamma}_D$ used here, or some value (from extrapolation of the flow curve) in the second case. Further comparison thus remains open to discussion.

5.3 Role of polydispersity

In the framework of the present model, it appears obvious that polydispersity should significantly increase the compactness of compact-SUs, for instance by adding small particles to a suspension of large particles that renders more difficult the dilatancy transition, although the cause might be very different in cases (a) — hydroclustering — and (b) — formation of dilated-SUs—. The presence of small particles could either decrease the effective value of Pe in the former case, or raise the cohesion of compact-SUs in the latter.

The same conclusions were recently drawn from experiments on bimodal dispersions in which the stress required for the onset of dilatancy was found to increase with the ratio of small to large particles [11,17]. Note that these results clearly give an additional argument that ODT is not required for shear thickening, as particle mixing should render difficult the formation of an ordered phase.

[14] Note that $\dot{\gamma}_D$ also depends on the particle radius through $\dot{\gamma}_C$, involved in ϕ_{m1} and ϕ_{m2} — see (3.3a and 3.3b) —. However, this dependence is negligible in comparison with that due to t_b, especially for very small particles.

The role of varying the polydispersity has been experimentally studied in water-coal dispersions [28]. A progressive reduction of dilatancy is observed, especially the disappearance of the viscosity discontinuity and its change into a viscosity maximum if the average size of particles (correlated with an increase in polydispersity) is large enough. Once again, these results could be interpreted as resulting from an enhancement of the SUs' compactnesses, φ_a and φ_b, more especially the latter that lowers ϕ_{m2} and increases ϕ_{m1}. A more quantitative study is in progress.

5.4 Role of the continuous phase viscosity

Analysis of Boersma *et al.*'s results (see Fig.6 in [5]) shows that the effect of decreasing η_F is a displacement of the whole curve towards higher shear rates rather than a lowering of the onset of dilatancy. This is in complete agreement with early empirical findings ([29] for ex.) which demonstrated that the viscosity data measured on different dispersions collapses on a single curve, η_R *vs.* $\eta_F\dot{\gamma}$, if instead of $\dot{\gamma}$ the product $(\eta_F\dot{\gamma})$ was used as a unique variable .

This feature is herein straightforwardly predicted if one takes into account the dependences of the characteristic times, t_a and t_b as functions of η_F. In the same way as ratios of the type $W_H/W_I = t_I\dot{\gamma}$, see (Part I, Eq. (3.5)), all products of $\dot{\gamma}$ with these times should be proportional to η_F, which leads to the critical shear rates (as reciprocals of characteristic times) $\dot{\gamma}_C$, $\dot{\gamma}_D$ and $\dot{\gamma}_M$ varying as $(\eta_F)^{-1}$. Therefore, at a given volume fraction, a master curve for the relative viscosity, $\eta_R = \eta_R(\phi,\ Pe)$, should be obtained in terms of the Péclet number, $Pe = t_a\dot{\gamma}$, with critical values $Pe_C = t_a\dot{\gamma}_C$, $Pe_D = t_a\dot{\gamma}_D$ and $Pe_M = t_a\dot{\gamma}_M$, which do not depend on η_F, see (3.2, 3.5) and (3.6). Figure 5b shows that indeed a single master curve (one for each ϕ-value) is obtained if one uses $\eta_F\dot{\gamma}$ instead of $\dot{\gamma}$.

6 Conclusion and perspectives

The description of shear thickening (dilatancy) in stabilized dispersions has been developed using the structural model [1] in which the presence of Structural Units (SUs) as transient clusters is postulated. In particular, the shear thinning behavior observed in the low shear domain prior to dilatancy at $\dot{\gamma} = \dot{\gamma}_C$ is described assuming a progressive (shear induced) disruption of large SUs considered as clusters (or clusters of clusters) of some basic units (either compact-SUs or primary particles).

Contrary to the "classical" interpretation of dilatancy based on the hypothesis of an Order Disorder Transition (ODT) — as a disruption of particle layering —, this novel approach assumes that dilatancy occurs at the level of SUs. More precisely, the onset of shear thickening at $\dot{\gamma}_C$ is assumed to result from stopping the SUs' breakup (at the

level of basic-SUs) and, beyond $\dot{\gamma}_C$, progressively promoting the hydrodynamic clustering recently demonstrated in both rheo-optical experiments and numerical simulations. Owing to the imprisonment of an increasing volume of continuous phase immobilized inside hydroclusters whose size grows as the shear rate increases, the EVF of the dispersion increases and so, does the viscosity.

Therefore, the suspension is described as a mixture of different classes of SUs depending on the shear rate domain. Especially in the dilatant domain, the populations of basic units and hydroclusters vary with the applied shear, resulting in an explicit expression for the whole effective volume fraction, $\phi_{\text{eff}}(\phi, \dot{\gamma})$, and thus for the viscosity. Using very simple assumptions — relaxation kinetics for describing the SUs' evolution and classical values for SUs' compactness —, this novel model allows calculation of the critical shear rates for onset of dilatancy, dilatancy maximum and discontinuous viscosity. Using realistic values of model variables, the model has been shown to be capable of predicting:

(i) the volume fraction dependences of these critical shear rates;
(ii) the effect of polydispersity;
(iii) the effect of continuous phase viscosity.

In good agreement with most of the observed characteristics of dilatancy that available models in literature did not describe up to now, even qualitatively. It appears quite remarkable that all these features (including those shown by rheograms at different volume fractions) have been well described despite the very simple assumptions on which the model is based, in particular those concerning the kinetics (only assumed to be of the relaxation type) governing the populations of basic-SUs and hydroclusters.

Due to these very simple assumptions, this model must be considered as a starting point in improving a more precise modeling based on better knowledge of the structural characteristics of the system, especially concerning the structure kinetics and a more precise evaluation of the critical shear rate at the onset of dilatancy. Note that a simple improvement of the model could be made by using more refined shear dependences in the kinetics constants without changing the basic features of the model. Moreover, it should be noted that this model could be extended to time dependent measurements, that is, to the description of antithixotropic materials, without adding any new ingredient. In fact, as already shown in Part I, the time-dependent viscosity $\eta(t) \equiv \eta[S_i(t)]$ under unsteady conditions directly results from the time dependent solutions of kinetic equations governing the structural variables, $S_i(t) = S_i[\dot{\gamma}(t), t]$. Therefore, it would be possible to obtain model predictions under unsteady conditions and to compare them with some experimental data, for instance the Kellers' data [28] on antithixotropic properties of coal-water dispersions. This work is in progress.

References

1. D. Quemada, Eur. Phys. J. AP **1**, 119 (1998).
2. D. Quemada, Eur. Phys. J. AP **2**, 175 (1998).
3. H.A. Barnes, J. Rheol. **33**, 329 (1989).
4. R.L. Hoffman, Trans. Soc. Rheol. **16**, 155 (1972).
5. R.L. Hoffman, J. Colloid Interface Sci. **46**, 491 (1974).
6. W.H. Boersma, J. Laven, H.N. Stein, AIChE J. **36**, 321 (1990).
7. W. Loose, S. Hess, Rheol. Acta **28**, 91 (1989).
8. B.J. Ackerson, P.N. Pusey, Phys. Rev. Lett. **61**, 1033 (1988).
9. B.J. Ackerson, J. Rheol. **34**, 553 (1990).
10. H.M. Laun, R. Bung, S. Hess, W. Loose, O. Hess, K. Hahn, E. Hädicke, R. Higmann, F. Schmidt, P. Linder, J. Rheol. **36**, 743 (1992).
11. P. d'Haene, J. Mewis, G.C. Fuller, J. Colloid Interface Sci. **156**, 350 (1993).
12. M.K. Chow, C.F. Zukoski, J. Rheol. **39**, 33 (1995).
13. W.J. Frith, P. d'Haene, R. Buscall, J. Mewis, J. Rheol. **40**, 531 (1996).
14. J.F. Brady, G. Bossis, Ann. Rev. Fluid Mech. **20**, 111 (1988).
15. G. Bossis, J.F. Brady, J. Chem. Phys. **91**, 1868 (1989).
16. L.J. Durlofsky, J.F. Brady, J. Fluid Mech. **200**, 39 (1989).
17. J.W. Bender, N.J. Wagner, J. Rheol. **40**, 899 (1996).
18. J.W. Bender, N.J. Wagner, J. Colloid Interface Sci. **172**, 171 (1995).
19. D. Quemada, in *Lect. Notes in Physics* **164**, edited by J. Casas-Vasquez and G. Lebon (Springer-Verlag, Berlin, 1982), p. 210.
20. C.G. de Kruif, E.M.F. van Iersel, A. Vrij, W.B. Russel, J. Chem. Phys. **83**, 4717 (1985).
21. I. Wagstaff, C.E. Chaffey, J. Colloid Interface Sci. **59**, 53 (1977).
22. D.S. Keller, D.V. Keller, Jr, J. Rheol. **34**, 1267 (1990).
23. D. Quemada, in *Proceedings of the XII International Congress on Rheology*, Québec, Canada (1996) p. 470.
24. O. Reynolds, Philos. Mag. **20**, 469 (1885).
25. W.B. Russel, *The Dynamics of Colloidal Systems* (The University of Wisconsin Press, London, 1987).
26. W.B. Russel, D.A. Saville, W.R. Schowalter, *Colloidal Dispersions* (Cambridge Univ. Press, 1989).
27. D.C.H. Cheng, R.A. Richmond, Rheol. Acta **17**, 446 (1978).
28. D.S. Keller, D.V. Keller, Jr, J. Rheol. **35**, 1583 (1991).
29. A. Eastwood, H.A. Barnes, Rheol. Acta **14**, 795 (1975).